Induced Pacemaker Activity in Virtual Mammalian Ventricular Cells

Wing Chiu Tong and Arun V. Holden

Computational Biology Laboratory, School of Biomedical Sciences,
University of Leeds, Leeds LS2 9JT, UK
cbs7wct@leeds.ac.uk
http://www.cbiol.leeds.ac.uk

Abstract. The stability of induced pacemaker activity in a virtual human ventricular cell is analysed by numerical simulations and continuation algorithms, with the conductance of the time independent inward rectifying potassium current (I_{K1}) as the bifurcation parameter. Autorhythmicity is induced within a narrow range of this conductance, where periodic oscillations and bursting behaviour are observed. The frequency of the oscillations approaches zero as the parameter moves towards the bifurcation point, suggesting a homoclinic bifurcation. Intracellular sodium ($[Na^+]_i$) and calcium ($[Ca^{2+}]_i$) concentration dynamics can influence the location of the bifurcation point and the stability of the periodic states. These two concentrations function as slow variables, pushing the fast membrane voltage system into and out of the periodic region, producing bursting behaviour. Moreover, suppressing I_{K1} will prolong action potential duration and may introduce risks of developing stable periodic intermittency and arrhythmia. A genetically engineered pacemaker may appear an attractive idea, but simple analysis suggests inherent problems.

1 Introduction

Cardiac pacemaker cells are autorhythmic, while ventricular cells are excitable and normally require repetitive current flows from neighbouring excited cells to generate repetitive action potentials. These contrasting behaviours are the sum of the activities of different membrane channels. Channel properties such as availability, density and single channel conductance, can be modelled as sets of maximum conductance for each current. Holden and Yoda [1, 2] have argued that the ionic channel densities of excitable cells can act as bifurcation parameters and these cells can undergo a Hopf bifurcation into autorhythmicity by a reduction in potassium conductance.

Indeed, pacemaker activity has been induced in mammalian ventricular cells. Miake et al [3, 4] injected a negative dominant gene construct of the Kir2.1 channels into ventricular myocytes of adult guinea pigs. The expression of the construct produced non-functional channels; as a result, the maximum conductance

A.F. Frangi et al. (Eds.): FIMH 2005, LNCS 3504, pp. 226–235, 2005.

($\bar{G}_{\mathrm{K1}}$) of the time independent inward rectifying potassium current (I_{K1}) was reduced. Cells with more than 80 % reduction in I_{K1} activity exhibited pacemaker activity; cells with moderate reduction had prolonged action potential duration (APD), depolarised resting membrane potential and reduced repolarisation rate. Over-expression of I_{K1} channels produced the opposite effects [4]. These studies suggest the possibility of genetically engineering a ventricular pacemaker by down-regulating I_{K1}.

Computational studies with ventricular cell models [5, 6] suggest that pacemaker activity induced by I_{K1} down regulation is carried by the sodium-calcium exchanger current (I_{NaCa}) and thus depends on intracellular sodium ($[\mathrm{Na}^{+}]_{\mathrm{i}}$) and calcium ($[\mathrm{Ca}^{2+}]_{\mathrm{i}}$) concentrations. As a consequence, the rate of the induced pacemaker activity may also respond to beta-adrenergic stimulation, as in natural pacemaker cells. Compared to the electronic pacemakers in clinical practice, a genetically engineered biological pacemaker that will not require surgical implantation and battery replacement every ten years, is regulated by the sympathetic nervous system, and can adapt to hormone changes, is an attractive idea.

However, for a functional pacemaker, stable periodic activity is crucial. Here we address this problem using numerical simulations and continuation algorithms to characterise the stability and bifurcations of the induced autorhythmic activities in a human ventricular cell model [7].

2 Human Ventricular Model

The human ventricular cell model by ten Tusscher et al [7] is used. For an isopotential single cell,

$$C_{\mathrm{m}} \frac{dV}{dt} = -I_{\mathrm{ion}} \ , \tag{1}$$

where V is the transmembrane potential (mV); I_{ion} is the total current density ($\mu\mathrm{A\,cm}^{-2}$), which is the sum of all currents of ion channels, pumps and exchangers; $C_{\mathrm{m}} = 2\,\mu\mathrm{F\,cm}^{-2}$, is the membrane specific capacitance. The equation was integrated using the forward Euler method with a variable time-step from 0.02 ms to 1 ms. The epicardial cell model, with parameters given in [7], was used so the results could be compared with other human epicardial cell models [8, 9]. In addition, an equivalent study was performed earlier using different cell types of the Luo-Rudy guinea pig ventricular cell model (LRd00) [10, 11]. Similar dynamics were observed among the cell types and their differences were marginal [12]. So, different cell types of the human model may also give similar results.

Down-regulation of I_{K1} was modelled by multiplying the standard value of $\bar{G}_{\mathrm{K1}}$ ($5.405\,\mathrm{nS\,pF}^{-1}$) with a dimensionless fractional term x, where $0 \leq x < 1$ represents suppression. In what follows, x is referred to as g_{K1}. When required, stimuli were applied with a current density of $-90\,\mathrm{pA\,pF}^{-1}$ for 0.5 ms, otherwise the cell was left unperturbed until steady state or periodic cycle was reached.

A solitary action potential evoked in the normal epicardial cell model and its restitution properties are illustrated in Fig. 1. Restitution is the relationship between action potential duration at 90 % repolarisation (APD_{90}) and diastolic

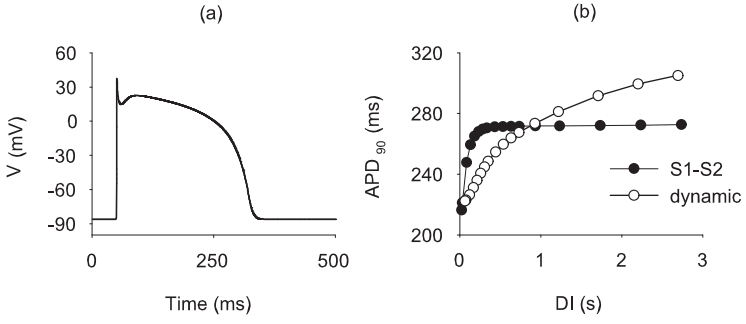

Fig. 1. (a) A solitary action potential excited by a stimulus in the epicardial cell model, $APD_{90} = 266$ms. (b) The S1-S2 restitution and the dynamic restitution

interval (DI), defined as the interval between the time at 90 % repolarisation of an action potential (AP) and the upstroke of the next AP. Two restitution protocols were used. S1-S2 restitution, a common method to define cellular properties, is found by applying a test stimulus (S2) at some DI after a train of 10 stimuli (S1) at 1 Hz. Dynamic restitution, which is more relevant to re-entry stability [13], is found by plotting the steady state APD_{90} against steady state DI during periodic pacing at different rates.

3 Down Regulation of I_{K1}

Pacemaker activity was induced in the human ventricular cell model. The membrane potential remained steady when I_{K1} was not suppressed ($g_{K1} = 1$) but autorhythmic action potentials appeared when I_{K1} was completely blocked ($g_{K1} = 0$) (Fig. 2a). The resting membrane potential depolarised as g_{K1} decreased; at $g_{K1} \approx 0.077$, i.e. $\sim 92\,\%$ reduction in I_{K1}, a bifurcation occurred separating the resting states and the oscillating states (Fig. 2b). Similar dynamics were also observed among different cell types of the LRd00 model: their bifurcation occurred at $g_{K1} \approx 0.3$, i.e. 70 % reduction in I_{K1} [12]. Therefore, a greater reduction in I_{K1} is required for pacemaker activity to be induced in human ventricular cells.

However, ventricular cells with down regulated I_{K1} may become proarrhythmic. In fact, patients with Andersen syndrome (OMIM: #170390)[1], where mutations in I_{K1} channels are implicated, may experience frequent periodic paralysis and ventricular arrhythmias [4, 6]. Stimulated at 1 Hz, APD_{90} is prolonged from 266 ms to 315 ms as g_{K1} decreases, and peaks at 345 ms at the bifurcation

[1] OMIM (Online Mendelian Inheritance in Man) is a database of human genes and genetic disorders. It can be accessed through the National Center for Biotechnology Information. http://www.ncbi.nlm.nih.gov/

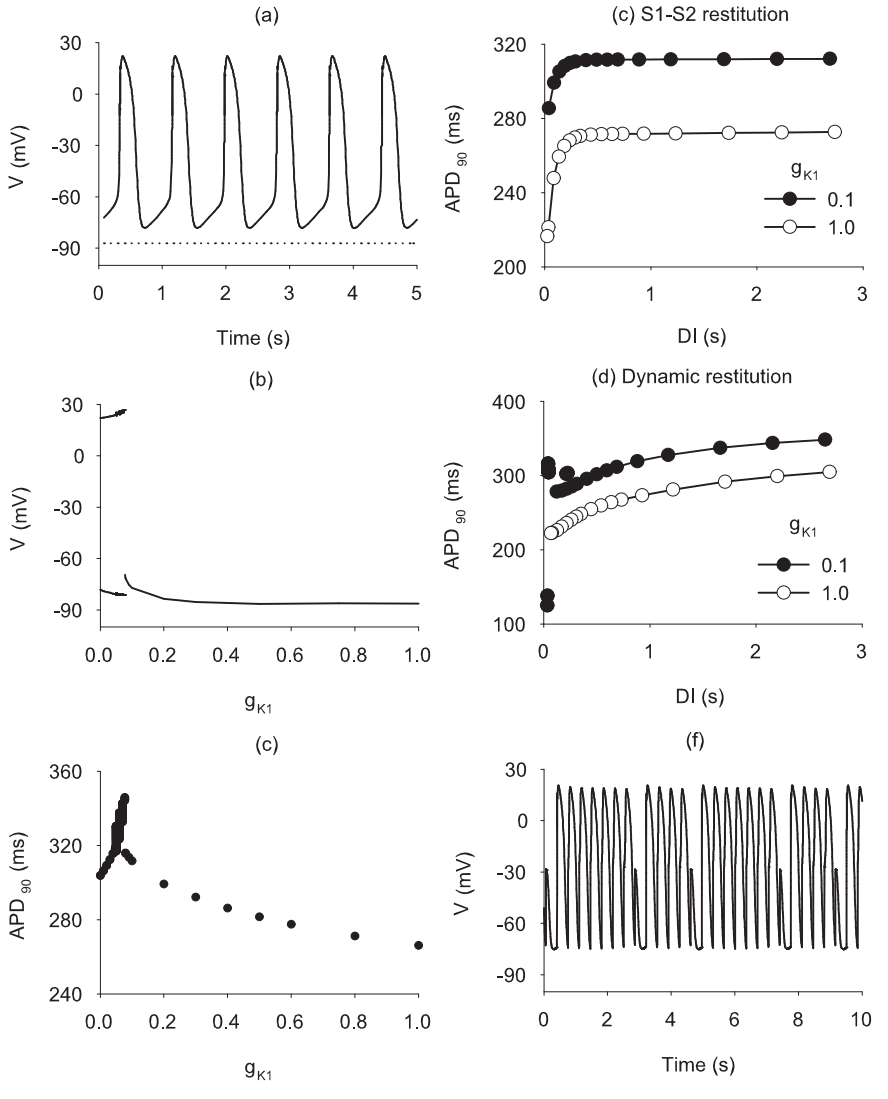

Fig. 2. (a) $V(t)$ with $g_{K1} = 0$ (*solid line*) and $g_{K1} = 1$ (*dotted line*) for the human epicardial cell model. Autorhythmicity is produced by complete block of I_{K1}. (b) The numerically computed bifurcation diagram with g_{K1} as the bifurcation parameter. The resting membrane potential depolarises as the parameter decreases and oscillations emerge at $g_{K1} \approx 0.077$. (c) Prolongation of APD_{90} with reducing g_{K1}. Where oscillations did not occur, steady state APD_{90} is determined by applying stimuli at 1 Hz. S1-S2 (d) and dynamic (e) restitutions of an epicardial cell model at $g_{K1} = 0.1$ and 1.0. Suppressing I_{K1} shifts both restitution curves upwards, and stable periodic intermittency is induced at small DI in dynamic restitution. (f) $V(t)$ of the intermittency after transients

point (Fig. 2c). Prolonged APD_{90} increases the time interval of the vulnerable window where extrasystoles may occur.

Moreover, suppressing I_{K1} alters the APD_{90} restitution properties, and may introduce a risk of developing stable periodic intermittency. At $g_{K1} = 0.1$, both the S1-S2 restitution (Fig. 2d) and the dynamic restitution (Fig. 2e) shifted upwards. Minimal change is found in the S1-S2 restitution. However, the dynamic restitution curve flattens when DI is less than 0.2 s and stable periodic intermittency develops for DI less than 50 ms. Fig. 2f shows an example of a stable periodic intermittency.

Down-regulation of I_{K1} in ventricular cell can push the cell from resting states into autorhythmic states, inducing pacemaker activity. However, potential risks for arrhythmogenesis increases as I_{K1} is suppressed, especially around the bifurcation point.

4 Bifurcation Analysis

For bifurcation analysis, continuation algorithms such as AUTO [14] – via XPPAUT [15] a simulation tool with an AUTO interface – is used in addition to the numerical experiments, to further characterise the behaviour and its stability of the human ventricular epicardial cell model. Continuation algorithms are useful for exploring the behaviour of a system, as they can trace solutions within parameter space, identify different types of bifurcation points and determine their stability.

AUTO requires the system to start from a steady state solution or a periodic orbit. However, the human ventricular cell model is a complex system with stiff, high-order differential equations. As the cell model is electrically but not electrochemically neutral [16], the full system could not settle into a stable steady state in XPPAUT. Therefore, a reduced system without intracellular concentration dynamics was used for continuation analysis in XPPAUT, as the intracellular concentration dynamics are slow compared to the fast membrane voltage system. The intracellular concentrations were clamped at constant values: $[Na^+]_i = 11.6$ mM; $[Ca^{2+}]_i = 0.2\,\mu$M; intracellular potassium, $[K^+]_i = 138.9$ mM. A fourth order Runge-Kutta integrator (within XPPAUT) with a fixed time step of 0.02 ms was used to bring the reduced system into steady state. Again, g_{K1} was set as the bifurcation parameter.

Solutions from the numerical experiments on the full system (Fig. 3a) show the system bifurcates at $g_{K1} \approx 0.077$, at which point periodicity and bursting occur. Oscillations emerge with large periods and quickly decrease with further reduction in g_{K1}. Moreover, these oscillations appeared to be stable over long period of time (80 min). This suggests a homoclinic bifurcation rather than a Hopf bifurcation.

AUTO solutions of the reduced system (Fig. 3b) show that it bifurcates in the non-physiological range at a negative g_{K1} with a Hopf bifurcation and high frequency (low period); and ends at a homoclinic bifurcation close to $g_{K1} \approx 0.05$ as the frequency approaches zero (infinite period). Compared to the full system in

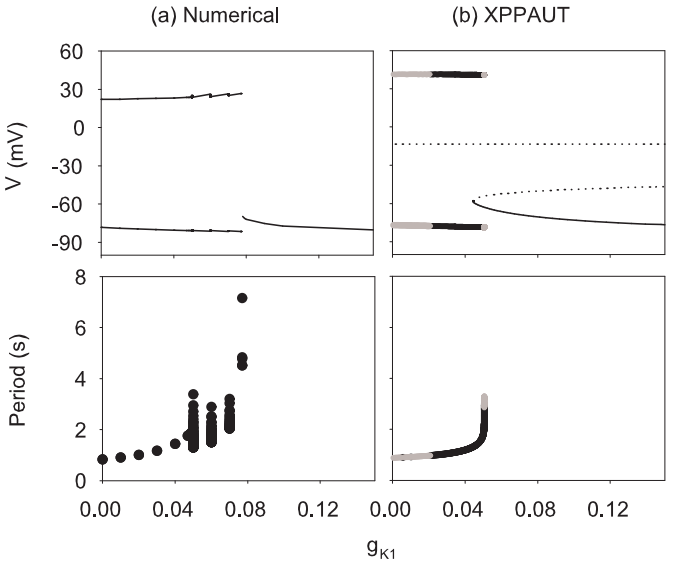

Fig. 3. Bifurcation diagrams with g_{K1} as the bifurcation parameter. (a) The full system with solutions computed numerically. Bifurcation point occurs at $g_{K1} \approx 0.077$. Periods are defined as the time interval between peaks (maximal V). In the range of g_{K1}: 0.05–0.077, multiple periods are observed and $V(t)$ shows bursting behaviour (see Fig. 4). (b) Stable (*black*) and unstable (*grey and dotted line*) solutions of the reduced system, which consists of only the fast membrane system and no intracellular ionic dynamics, are traced by the continuation algorithm, AUTO/XPPAUT. Only the physiological range of g_{K1} is shown. The bifurcation point occurs at $g_{K1} \approx 0.05$, less than the numerical solutions of the full system. Bursting is not seen in the reduced system

Fig. 3a, bursting is not observed in the reduced system. Also, stable oscillations only occur within a narrow range of g_{K1} and their stability is lost again when the system is close to the bifurcation point. Moreover, this bifurcation point coincides with the onset of bursting in the full system, suggesting that the dynamics of intracellular concentrations could influence the behaviour and stability of a virtual ventricular cell.

5 Bursting Behaviour

The bursting behaviour seen in the full system of the human ventricular cell is curious as it is common among neurons, smooth muscle, endocrine cells and embryonic cardiac cells [17, 18, 19, 20], but is rarely observed in adult cardiac myocytes. At $g_{K1} = 0.07$, $V(t)$ shows neuron-like bursting behaviour on a time scale of minutes with the action potential bursts repetitively interrupted by a long period of inactivity (Fig. 4a). The intervals between action potentials

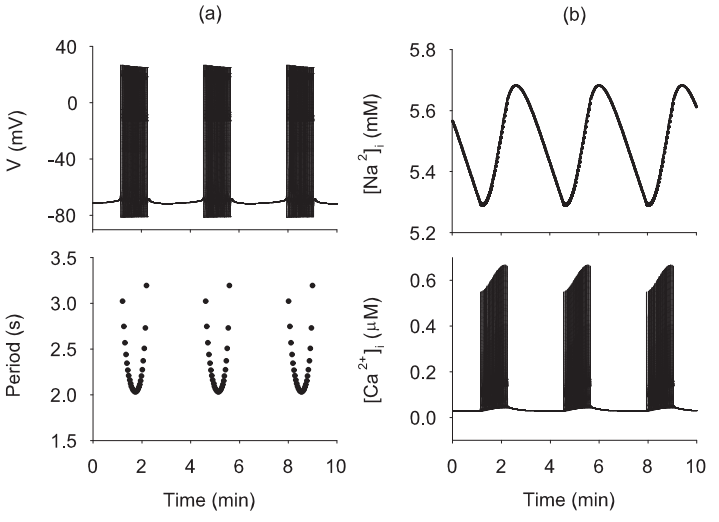

Fig. 4. Bursting behaviour of the full system seen at $g_{K1} = 0.07$ and after all the transients. (a) $V(t)$ shows periods of inactivity interrupting the oscillations (top). The periods of the oscillations follow a parabolic fashion (bottom). (b) Oscillations of $[Na^+]_i$ (top) and $[Ca^{2+}]_i$ (bottom) during bursting

decreases and increases during the bursting, and the action potentials undershoot below the voltage observed during the quiet period. These are characteristics of Type II parabolic bursting.

Type II bursting involves oscillations of at least two slow variables pushing the fast membrane system in and out of a homoclinic bifurcation [21, 22, 23]. As the intracellular concentration dynamics are slow compared to the fast membrane voltage system, these could be the variables that drive the bursting behaviour in the full system of the human ventricular cell model. We focused on $[Na^+]_i$ and $[Ca^{2+}]_i$ in particular as the pacemaker activity was suggested to be carried by I_{NaCa} [5]. Fig. 4b shows oscillations of $[Na^+]_i$ and $[Ca^{2+}]_i$ during bursting, and Fig. 5a shows that these concentrations form an orbit in the phase diagram, where bursting starts at low $[Na^+]_i$ and $[Ca^{2+}]_i$ and terminates as these concentrations accumulate.

In order to determine the dynamics of the fast membrane system with different combinations of intracellular concentrations, a two parameter bifurcation diagram with $[Na^+]_i$ and $[Ca^{2+}]_i$ as bifurcation parameters is computed at $g_{K1} = 0.07$ with XPPAUT and the reduced system of the human ventricular cell model (Fig. 5b). The left arm (between 5 mM of $[Na^+]_i$ and the cusp point) separates periodic and steady states solutions of the fast membrane system. The base of this arm swings from left to right as g_{K1} is reduced (not shown). In spite of the dynamics of this boundary, for stable steady solutions, the full system is represented by a point underneath the arm; for stable periodicity, the full system forms a single $[Na^+]_i$-$[Ca^{2+}]_i$ orbit above the arm.

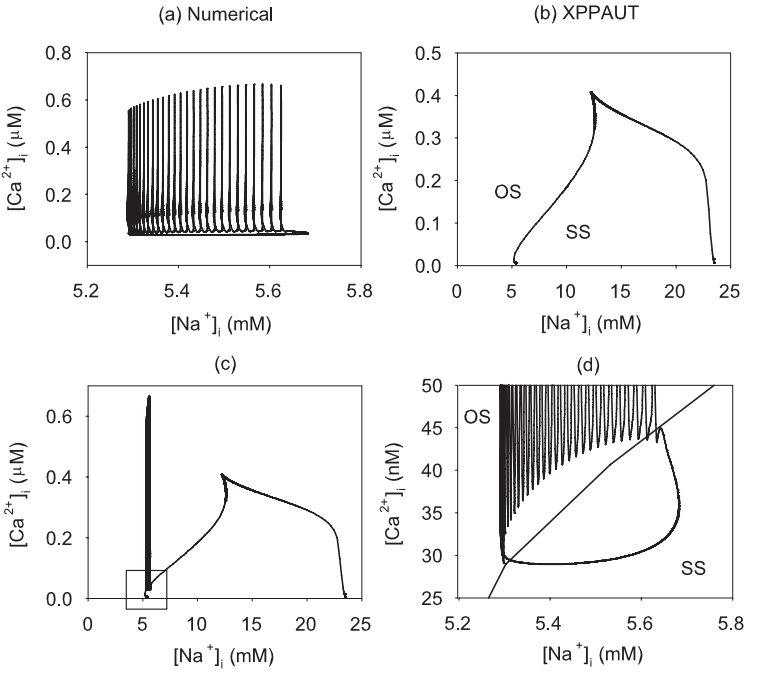

Fig. 5. (a) Numerical results of the dynamics between intracellular sodium ($[Na^+]_i$) and calcium ($[Ca^{2+}]_i$) concentrations during bursting in the full system at $g_{K1} = 0.07$. Bursting starts at low $[Na^+]_i$ and $[Ca^{2+}]_i$ and terminates as these concentrations accumulate. (b) Two parameter bifurcation diagram computed by XPPAUT using the reduced system at $g_{K1} = 0.07$. The arm between 5 mM of $[Na^+]_i$ and the cusp point separates steady states (*SS*) and the oscillatory states (*OS*) of the fast membrane system. (c) Superimposed the numerical results in (a) onto the two parameter bifurcation diagram in (b), the full system is right on the boundary between periodic and steady states. The details in the box are shown enlarged in (d). The full system is being pushed across and back from the boundary by $[Na^+]_i$ and $[Ca^{2+}]_i$ dynamics. Bursting starts clockwise as the system enters the *OS* region and terminates when it falls back into the *SS* region but unable to push across the boundary again

Superimposing the $[Na^+]_i$-$[Ca^{2+}]_i$ orbit during bursting in Fig. 5a onto the two parameter bifurcation diagram in Fig. 5b shows that at $g_{K1} = 0.07$, where bursting occurs, the system is on the boundary of periodic and steady states (Fig. 5c and Fig. 5d). Bursting initiates when both $[Na^+]_i$ and $[Ca^{2+}]_i$ are low. $[Ca^{2+}]_i$ accumulates much faster than $[Na^+]_i$ initially, pushing the system away from the boundary. However, as more $[Na^+]_i$ accumulates, the system is pushed back towards the boundary and eventually crosses the boundary into the steady states region.

Intracellular concentration dynamics are not only responsible for the bursting behaviour in the human ventricular cell model, but could also influence the location of the bifurcation point of g_{K1} and the stability of the pacemaker activ-

ity. For example, with higher $[Na^+]_i$, the bifurcation point of g_{K1} in the reduced system will shift to the right, but the oscillations become more unstable; with lower $[Na^+]_i$, the bifurcation point will shift to the left, but the oscillations with become more stable (results not shown).

6 Conclusion

Pacemaker activity induced in human virtual ventricular cells is addressed here using both numerical simulations and continuation algorithms. Autorhythmicity is induced within a very narrow range of g_{K1} (0–0.077), implying that more than 92 % block of I_{K1} may be required to induce pacemaker activity in human ventricular cells. Within this narrow range, less than two thirds of the g_{K1} (0–0.05) show apparent stable periodic oscillations, the remainder exhibiting bursting behaviour. Application of continuation algorithms to a reduced system without slow intracellular concentration dynamics shows that the range of g_{K1} for stable autorhythmicity is further restricted to $g_{K1} = 0.02$–0.05.

Intracellular concentration dynamics plays a critical role in the behaviour and stability of the induced autorhythmicity in ventricular cells. For example, the observed bursting behaviour is a product of the slow dynamics of intracellular concentrations driving the fast membrane system between periodic and steady states. Therefore, manipulating intracellular concentrations, maybe via the activities of the sodium-potassium pump and the sodium-calcium exchanger, could be tools to influence the stability and behaviour of the induced autorhythmicity in human ventricular cells.

In addition to the stability of induced pacemaker activity, suppressing I_{K1} in human ventricular cell will prolong APD_{90} and introduce risks of developing stable periodic intermittency and arrhythmia. The genetically engineered pacemaker suggested by Miake et al [3] may appear an attractive idea, but simple analysis suggests inherent problems.

WCT is supported by a British Heart Foundation research studentship (FS/03/075/15914).

References

1. Holden, A.V., Yoda, M.: Ionic channel density of excitable-membranes can act as a bifurcation parameter. Biol. Cyber. **42** (1981) 29-38
2. Holden, A.V., Yoda, M.: The effects of ionic channel density on neuronal function. J. Theor. Neurobiol. **1** (1981) 60-81
3. Miake, J., Marban, E., Nuss, H.B.: Biological pacemaker created by gene transfer. Nature **419** (2002) 132-133
4. Miake, J., Marban, E., Nuss, H.B.: Functional role of inward rectifier current in heart probed by Kir2.1 over expression and dominant-negative suppression. J. Clin. Invest. **111** (2003) 1529-1536
5. Silva, J., Rudy, Y.: Mechanism of Pacemaking in IK1-downregulated myocytes. Circ. Res. **92** (2003) 261-263

6. Tristani-Firouzi, M., Jensen, J.L., Donaldson, M.R., Sansone, V., Meola, G., Hahn, A., Bendahhou, S., Kwiecinski, H., Fidzianska, A., Plaster, N., Fu, Y.H., Ptacek, L.J., Tawil, R.: Functional and clinical characterization of KCNJ2 mutations associated with LQT7 (Andersen syndrome). J. Clin. Invest. **110** (2002) 381-388
7. ten Tusscher, K.H.W.J., Noble, D., Noble, P.J, Panfilov, A.V.: A model for human ventricular tissue. Am. J. Physiol. **286** (2004) H1573-H1589
8. Iyer, V., Mazhari, R., Winslow, R.L.: A Computational Model of the Human Left-Ventricular Epicardial Myocyte. Biophys. J. **87** (2004) 1507-1525
9. Priebe, L., Beuckelmann, D.J.: Simulation Study of Cellular Electric Properties in Heart Failure. Circ. Res. **82** (1998) 1206-1223
10. Faber, G.M., Rudy, Y.: Action potential and contractility changes in [Na+](i) overloaded cardiac myocytes: a simulation study. Biophys. J. **78** (2000) 2392-2404
11. Faber, G.M.: The Luo-Rudy dynamic model of mammalian ventricular action potential. (2000) http://www.cwru.edu/med/CBRTC/LRdOnline/
12. Benson, A.P., Tong, W.C., Holden, A.V., Clayton, R.H.: Induction of autorhythmicity in virtual ventricular myocytes and tissue. J. Physiol. (Proceedings). (2005) (to appear)
13. Koller, M.L., Riccio, M.L., Gilmour, R.F. Jr.: Dynamic restitution of action potential duration during electrical alternans and ventricular fibrillation. Am. J. Physiol. Heart. Circ. Physiol. **275** (1998) H1635-H1642
14. Doedel, E.J.: AUTO: A program for the automatic bifurcation and analysis of autonomous systems. Cong. Num. **30** (1981) 265-284
15. Ermentrout, G.B.: XPPAUT. http://www.math.pitt.edu/∼bard/xpp/xpp.html
16. Hund, T.J., Kucera, J.P., Otani, N.F., Rudy, Y.: Ionic charge conservation and long-term steady state in the Luo-Rudy dynamic cell model. Biophys. J. **81** (2001) 3324-3331
17. Bub, G., Glass, L., Publicover, N.G., Shrier, A.: Bursting calcium rotors in cultured cardiac myocyte monolayers. Proc. Natl. Acad. Sci. U. S. A. **95** (1998) 10283-1.0287
18. Cohen, N., Soen, Y., Braun, E.: Spatio-temporal dynamics of networks of heart cells in culture. Physica. A. **249** (1998) 600-604
19. Cohen, N.: The development of spontaneous beating activity in cultured heart cells: From cells to networks. PhD thesis, Technion – Israel Institute of Technology. (2001)
20. Soen, Y., Cohen, N., Braun, E., Lipson, D.: Emergence of spontaneous rhythm disorders in self-assembled networks of heart cells. Phys. Rev. Lett. **82** (1999) 3556-3559
21. Bertram, R., Butte, M., Kiemel, T., Sherman, A.: Topological and Phenomenological Classification of Bursting Oscillations. Bull. Math. Biol. **57** (1995) 413-439
22. Rinzel, J., Ermentrout, B.: Analysis of neural excitability and oscillations. In: Koch, C., Segev, I. (eds.): Methods in Neuronal Modeling: From Synapses to Networks, 2nd eds. MIT Press, Cambridge, MA (1999) 251-292
23. Wang, X.-J., Rinzel, J.: Oscillatory and bursting properties of neurons. In: Arbib, M.A. (ed.): Handbook of brain theory and neural networks. MIT Press, Cambridge, MA (1995) 686-691